

Generation of tholeiitic and calc-alkaline arc magmas and its implications for continental growth

Kang Chen^{a,*}, Ming Tang^b, Zhaochu Hu^a, Yongsheng Liu^{a,c}

^a State Key Laboratory of Geological Processes and Mineral Resources, China University of Geosciences, Wuhan 430074, China

^b Key Laboratory of Orogenic Belt and Crustal Evolution, School of Earth and Space Sciences, Peking University, Beijing 100871, China

^c School of Earth Sciences, China University of Geosciences, Wuhan 430074, China

ARTICLE INFO

Associate editor: Adam Simon

Keywords:

Arc magma differentiation
Magnetite fractionation
Crustal thickness
Garnet fractionation
Continental crust formation

ABSTRACT

Arc magmas, the building blocks of the Phanerozoic continents, are compositionally diverse. The most prominent compositional diversity is that some arcs show early Fe enrichment while some others show the opposite trend. What causes this Fe differentiation diversity is important for understanding continent formation but remains highly debated. Here, we use pressure-sensitive geochemical proxies, combined with experimental results, to evaluate the petrological mechanism(s) for the different Fe trends in arc magmas that traverse through crusts of various thicknesses. We show that magnetite starts to fractionate only at $\text{MgO} \leq 4 \text{ wt}\%$ for nearly all arc magmas and thus has no bearing on the early Fe depletion in calc-alkaline arc magmas. The Fe enrichment at $\text{MgO} > 4 \text{ wt}\%$ for tholeiitic arc magmas is largely caused by clinopyroxene fractionation. The culprits for the Fe depletion at $\text{MgO} > 4 \text{ wt}\%$ in calc-alkaline arc magmas change from pyroxene- to garnet-dominated (\pm amphibole) as the arc crust thickens. The similarity between the upper continental crust and the calc-alkaline arc magmas suggests that calc-alkaline arc magmas are an essential component for the continental crust. The high La/Yb and Dy/Yb estimates for the average upper continental crust imply that garnet fractionation is an intrinsic feature of the upper continental crust. Thus, crustal thickness, that is differentiation pressure, exerts a first-order control on arc magma compositions and high-pressure intracrustal differentiation in thickened crust is necessary for making the Phanerozoic continental crust.

1. Introduction

Arc magmatism in subduction zones is widely thought to play a critical role in the formation and growth of the continental crust (Taylor and White, 1965; Taylor, 1977; Weaver and Tarney, 1982; Rudnick, 1995). Yet, there is large compositional diversity in arc magmas, presenting a major challenge for understanding of the nature of arc magmas and the origin of the continental crust. The most prominent compositional diversity is reflected in the distinct Fe trends during the differentiation of different arc magmas. In some arcs, magmas show initial Fe enrichment and late depletion during differentiation, a defining feature of tholeiitic magma series, while some other arc magmas are characterized by continuous Fe depletion during differentiation, pertaining to calc-alkaline magma series (Irvine and Baragar, 1971; Miyashiro, 1974). Other arc magmas possess transitional Fe trends. The petrological mechanism causing the various Fe differentiation trends during arc magma evolution is still highly debated.

The debate is centered on which mineral(s) cause the initial Fe depletion in calc-alkaline arc magmas. One school of thought attributes the initial Fe depletion in calc-alkaline magmas to magnetite fractionation. This viewpoint is supported by some experiments showing that the hydrous and oxidized nature of arc magmas would suppress plagioclase (a Fe-poor mineral) saturation and enhance magnetite fractionation (Osborn, 1959; Sisson and Grove, 1993; Botcharnikov et al., 2008; Hamada and Fujii, 2008; Zimmer et al., 2010). However, this cannot explain why some arc magmas differentiate along trends of Fe-enrichment initially. An alternative explanation suggests that garnet (\pm amphibole) fractionation results in the early Fe depletion in calc-alkaline magmas (Green and Ringwood, 1967, 1968a, b; Cawthorn and O'Hara, 1976; Huang and Wyllie, 1986; Larocque and Canil, 2010; Chapman et al., 2016; Tang et al., 2018; Barber et al., 2021; Du et al., 2022). This explanation is supported by the observation that calc-alkaline magmas principally occur in arcs with thick crusts (e.g., $>30\text{--}40 \text{ km}$) where thick arc crusts result in high differentiation

* Corresponding author.

E-mail address: kangchen@cug.edu.cn (K. Chen).

<https://doi.org/10.1016/j.gca.2023.07.002>

Received 8 January 2023; Accepted 2 July 2023

Available online 4 July 2023

0016-7037/© 2023 Elsevier Ltd. All rights reserved.

pressures and enhance garnet (\pm amphibole) fractionation while tholeiitic magmas dominate in arcs with thin crusts (Miyashiro, 1974; Green, 1982). The role of high-pressure differentiation in affecting magma Fe contents is further shown by the positive correlation between the degree of Fe depletion and the arc crust thickness (Farner and Lee, 2017; Tang et al., 2018).

In the foregoing two scenarios, the early fractionated minerals are different, which will impart distinct geochemical signatures to the derivative melts. For example, Fe, Ti, Mn, and V are all compatible in magnetite (Toplis and Corgne, 2002), so magnetite fractionation will cause the simultaneous reduction of the melt Fe, Ti, Mn, and V contents. Magma FeO_T/MnO (FeO_T is the total Fe as FeO) can also be lowered by magnetite fractionation due to the high $D_{\text{Fe}}/D_{\text{Mn}}$ (D , partition coefficient) in magnetite (~ 10), whereas fractionation of olivine, clinopyroxene, orthopyroxene, garnet, and amphibole has little influence on magma FeO_T/MnO because these minerals have $D_{\text{Fe}}/D_{\text{Mn}}$ near unity (0.6–1.6, Fig. 1, Table S1). The ratios of light and middle to heavy rare earth elements (REEs) are often used to track garnet and amphibole fractionation (e.g., La/Yb, Dy/Yb, Gd/Yb, Rudnick and Taylor, 1986; Davidson et al., 2007). Garnet preferentially incorporates heavy REEs, resulting in increases of magma La/Yb and Dy/Yb upon differentiation. Amphibole, and to a lesser extent, clinopyroxene preferentially incorporate middle REEs relative to heavy REEs, giving rise to slight increase of La/Yb and mild decrease of Dy/Yb in the derivative magmas (Fig. 1). REEs are highly incompatible in olivine, orthopyroxene, and magnetite, so their fractionation has little effect on REE ratios of the melt.

To decipher the petrological mechanism for the different Fe differentiation trends in arc magmas, we use FeO_T , TiO_2 , MnO, V, FeO_T/MnO , La/Yb, and Dy/Yb in Cenozoic volcanic rocks from global magmatic arcs to trace the fractionation of Fe-rich minerals, including magnetite, garnet, and amphibole. The fractionated mineral assemblages that caused the Fe enrichment in tholeiitic arc magmas and the Fe depletion in calc-alkaline arc magmas are deduced using these geochemical

proxies, together with the results from hydrous experiments conducted under similar pressure conditions. We then compare these geochemical proxies of the average continental crust with different arc magmas to assess the roles different magmatic arcs played in the formation and growth of the Phanerozoic continental crust.

2. Materials and methods

We compile geochemical compositions of Cenozoic volcanic rocks from 22 magmatic arcs worldwide from the GEOROC database. Details for the 22 arcs are given in Table S2. Among them, Bismarck, Izu-Bonin, Lesser Antilles, Mariana, New Hebrides, Ryukyu, Tonga, and Western Aleutian are type examples of oceanic arcs. Cascades, Central American Volcanic Belt, New Zealand, Mexican Volcanic Belts, and the Northern, Central, and Southern Volcanic Zones from the Andes are typical continental arcs. We filtered the compiled whole rock data by removing samples named as a mantle-type rock (e.g., peridotite), marked as “Extensively, Moderately or Slightly Altered”, listed as a back-arc or ridge location, or reported with major element oxide sums out of the range of 97.5–101.5 wt%. Then the samples after filtering are plotted in GeoMapApp (<https://www.geomapapp.org>) by their coordinates to check if the samples are indeed collected from the corresponding arc areas. Bulk rock compositions for statistical computing after filtering (about 30,000 samples) are provided in Table S3.

3. Results

To present the compiled data in a simple and clear manner, we divide magmatic arcs into three groups based on the early Fe trends during arc magma differentiation: Fe-enriching arcs (tholeiitic magma series), Fe-depleting arcs (calc-alkaline magma series), and transitional arcs between the former two groups (transitional magma series). It should be noted that there are no distinct boundaries between different groups and

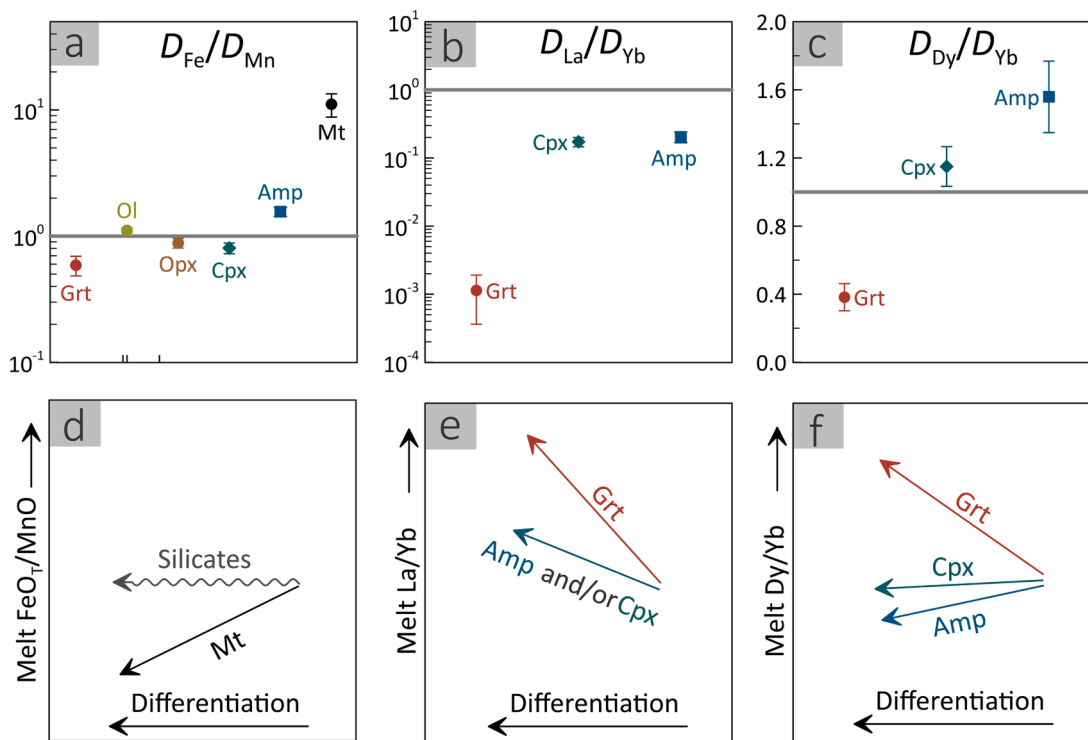


Fig. 1. Partition coefficients for the geochemical proxies (a, b, and c) and the effects on these proxies in magmas from differentiation (d, e, and f). Data for D_{Fe} and D_{Mn} are from the compilation by Tang et al. (2020). Data for D_{La} , D_{Dy} , and D_{Yb} are compiled from the Geochemical Earth Reference Model (GERM, <https://kdd.earth.ref.org/Kdd/>) and provided in Table S1. It should be noted that the D values are only used in a schematic way here to produce the general trends for the three ratios in melts. Mineral abbreviations: Ol, olivine; Opx, orthopyroxene; Cpx, clinopyroxene; Grt, garnet; Amp, amphibole; Mt, magnetite.

natural arc magmas span continuously from Fe-enriching to Fe-depleting differentiation series. Traditionally, the FAM diagram (FeO_T versus $(\text{Na}_2\text{O} + \text{K}_2\text{O})$ versus MgO) recommended by Irvine and Baragar (1971) or the SiO_2 versus FeO_T/MgO diagram advocated by Miyashiro (1974) are commonly used to distinguish between the two magma series. More recently, the FeO_T versus MgO diagram has also been used to define the two magma series by many researchers (Zimmer et al., 2010; Chiaradia, 2014; Keller et al., 2015; Grove and Brown, 2018; Tang et al., 2018; Ulmer et al., 2018; Barber et al., 2021). We argue that the FeO_T versus MgO diagram is a more straightforward, simpler, and equally effective way in discriminating between tholeiitic and calc-alkaline magma series.

To quantitatively assess the degree of early Fe enrichment or depletion during arc magma differentiation, we use $\text{Fe}_{5.0}/\text{Fe}_{8.0}$, where $\text{Fe}_{5.0}$ is the average FeO_T contents of samples with 4–6 wt% MgO because we find that some arc magmas show highest FeO_T at MgO = 4–6 wt% (Fig. S1), and $\text{Fe}_{8.0}$ is the average FeO_T at 7–9 wt% MgO. $\text{Fe}_{5.0}/\text{Fe}_{8.0}$ is similar to the Tholeiitic Index (THI) proposed by Zimmer et al. (2010). In their work, THI was defined as $\text{Fe}_{4.0}/\text{Fe}_{8.0}$, where $\text{Fe}_{4.0}$ is the average FeO_T contents of samples with 3–5 wt% MgO, and $\text{Fe}_{8.0}$ is the average FeO_T at

7–9 wt% MgO. Because there are sharp decreases of Fe with decreasing MgO at MgO interval of 3–4 wt% in most of the arcs (Figs. S1, S2 and S3), the calculation of their THI will cover large amounts of low-Fe samples with MgO = 3–4 wt%, and thus underestimates the degree of early Fe enrichment. For example, Honshu and Kamchatka show constant average FeO_T contents at MgO > 4 wt% (Fig. S2), so magmas from these arcs should be grouped into the transitional arc group. But the THI from Zimmer et al. (2010) of these arc magmas are 0.90 and 0.92, respectively, making them calc-alkaline magma series. This is contradictory to the traditional definition of calc-alkaline magma series that calc-alkaline magmas show an FeO_T decrease in the initial differentiation stage (Irvine and Baragar, 1971; Miyashiro, 1974).

We assume that a $\text{Fe}_{5.0}/\text{Fe}_{8.0}$ of 0.95–1.05 implies neither obvious Fe enrichment nor obvious Fe depletion, and thus arcs with $\text{Fe}_{5.0}/\text{Fe}_{8.0}$ of 0.95–1.05 are divided into the transitional magma series. Arcs with $\text{Fe}_{5.0}/\text{Fe}_{8.0} > 1.05$ show Fe enrichment during the early differentiation stage, and thus are the tholeiitic magma series. Arcs with $\text{Fe}_{5.0}/\text{Fe}_{8.0} < 0.95$ are characterized by early Fe depletion and are grouped into the calc-alkaline magma series. The results of the grouping are listed in Table S2. In this study, we will only focus on the formation mechanisms

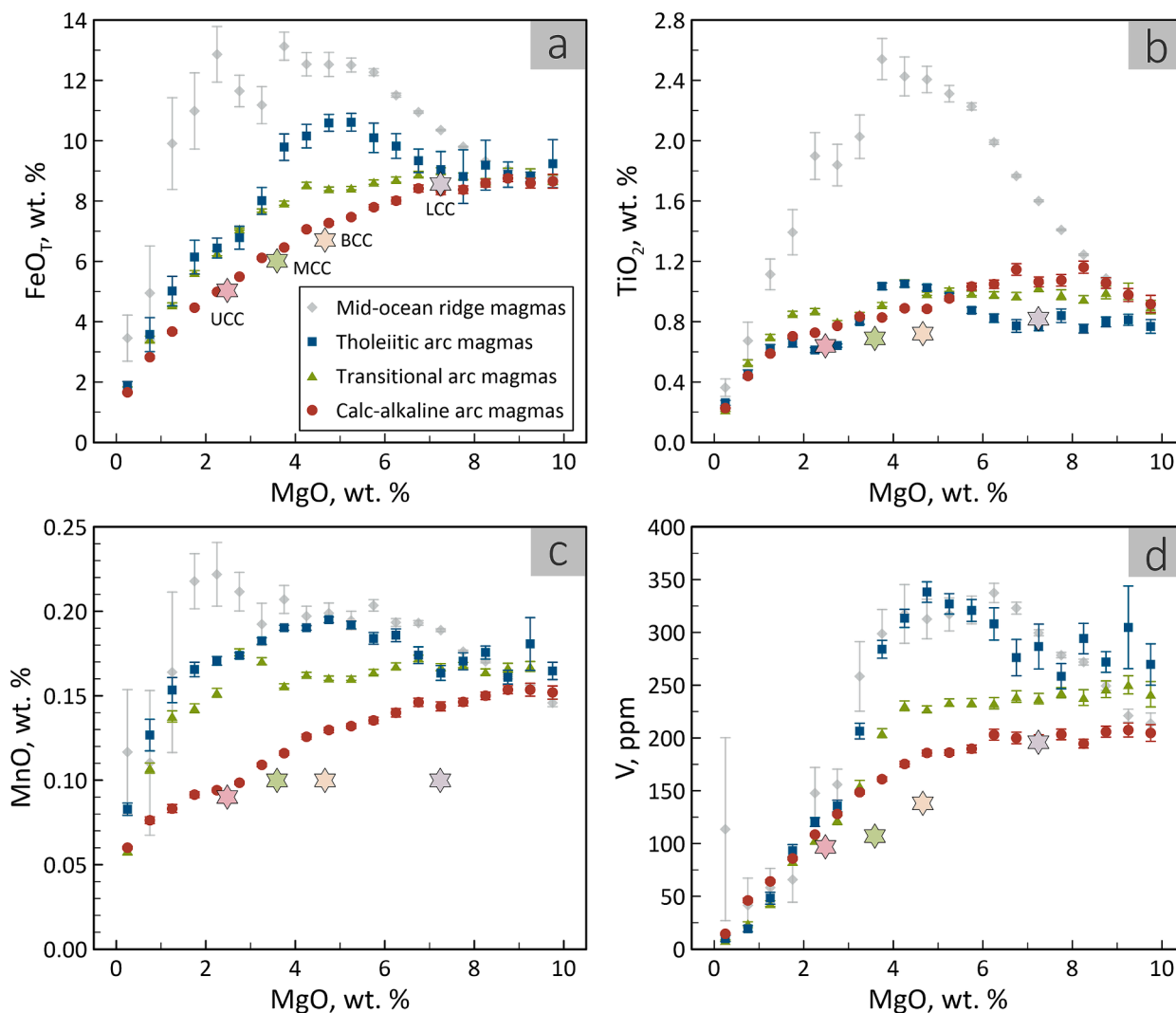


Fig. 2. FeO_T , TiO_2 , MnO, and V differentiation trends in magmas from global magmatic arcs and mid-ocean ridges. Data are binned by 0.5 % MgO content, and within each bin, the mean values of FeO_T , TiO_2 , MnO, and V and the two standard errors are plotted. For each MgO bin, we removed 10% of the samples with the highest values and 10% with the lowest values to alleviate the influence of outliers on the averages. BCC, UCC, MCC, and LCC denote bulk, upper, middle, and lower continental crust, respectively, and the abundance estimates are from Rudnick and Gao (2003). Note the synchronous turning points of the four elements from increasing to decreasing at MgO = 4–5 wt% in tholeiitic arc magmas, indicative of the start of magnetite fractionation at this point. The results of individual arcs are presented in Figs. S1–S3. Arc magma data are provided in the Table S3. Mid-ocean ridge magma data are from Keller et al. (2015).

of the Fe trends in the tholeiitic and the calc-alkaline magma series.

The average trends of FeO_T , TiO_2 , MnO , and V , and FeO_T/MnO for the three groups during arc magma differentiation are plotted in Figs. 2 and 3, respectively. The average trends of La/Yb and Dy/Yb are plotted in Fig. 4, with the calc-alkaline arc magmas represented by those differentiated under two end member pressure conditions (see Section 4.2). Results for individual arcs are plotted in Figs. S1–S6. In the tholeiitic arc magmas, FeO_T content first increases with decreasing MgO and then starts to decrease at $\text{MgO} = 4\text{--}5\text{ wt}\%$, the defining feature of the tholeiitic magma series (Irvine and Baragar, 1971; Miyashiro, 1974). The contents of TiO_2 , MnO , and V show similar trends with FeO_T . The FeO_T/MnO remains unchanged at $\text{MgO} > 4\text{--}5\text{ wt}\%$ and then starts to decrease from this point. The tholeiitic arcs have systematically lower La/Yb and Dy/Yb ratios than the transitional and the calc-alkaline arcs. By contrast, for calc-alkaline arc magmas, the FeO_T content continuously decreases during the entire differentiation path, the defining feature of the calc-alkaline magma series (Irvine and Baragar, 1971; Miyashiro, 1974). However, we find no synchronous decreasing of the five proxies at $\text{MgO} > 4\text{ wt}\%$ in Figs. 2 and 3. For example, the V content and FeO_T/MnO in calc-alkaline arcs remain generally invariable at $\text{MgO} > 4\text{ wt}\%$. Calc-alkaline arcs are characterized by apparently higher La/Yb and Dy/Yb than the transitional and tholeiitic arcs, with the high-pressure calc-alkaline arcs having higher values than the medium-pressure ones (see Section 4.2).

4. Discussion

4.1. Magnetite fractionation

Magnetite fractionation significantly reduces magma Fe contents. For example, 1 wt% fractionation of magnetite would scavenge $\sim 10\%$ Fe of a magma with 10 wt% FeO_T . To understand the mechanism of the different Fe trends in arc magmas, we first investigate the timing of magnetite fractionation during arc magma differentiation.

For tholeiitic arc magmas, magnetite is not saturated when MgO is $> 4\text{--}5\text{ wt}\%$, as evidenced by the increasing of average contents of FeO_T , TiO_2 , MnO , and V with decreasing MgO (Fig. 2) and by the nearly constant FeO_T/MnO ratios (Fig. 3). At $\text{MgO} = 4\text{--}5\text{ wt}\%$, all the five

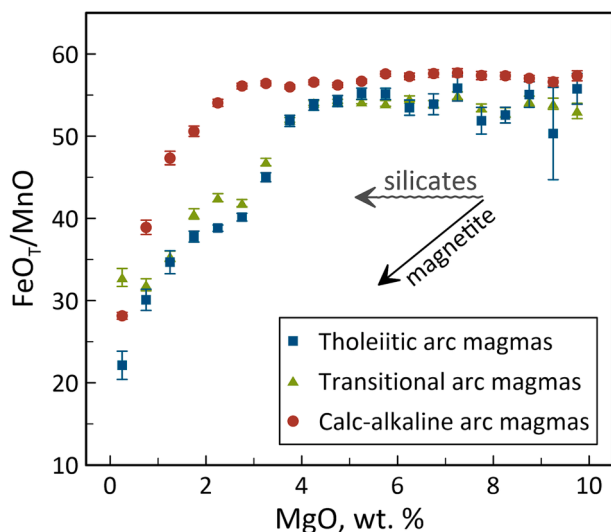


Fig. 3. FeO_T/MnO differentiation trends in magmas from global magmatic arcs. Data sources for arc magmas are provided in the Table S3. Data are binned by 0.5 % MgO content, and within each bin, the mean values of FeO_T/MnO and the two standard errors are plotted. For each MgO bin, we removed 10% of the samples with the highest values and 10% with the lowest values to alleviate the influence of outliers on the calculation of the averages. The results of individual arcs are presented in Figs. S4–S6.

proxies start to plummet, indicative of magnetite fractionation from this point. These proxies in individual tholeiitic arcs (Fig. S1) show similar trends with their global average trends, indicating that the global average trends shown in Figs. 2 and 3 can represent the differentiation features of global tholeiitic arc magmas. The fractionation of magnetite at intermediate differentiation stage is also supported by experimental studies. For example, when hydrous basaltic magmas differentiate under 0.7 GPa and redox conditions relevant to arc settings, magnetite only becomes saturated at 150–250 °C below the liquidus (e.g., Nandedkar et al., 2014). Thus, magnetite starts to fractionate at the intermediate stage ($\text{MgO} = 4\text{--}5\text{ wt}\%$) during the differentiation of tholeiitic arc magmas and plays a dominant role in the Fe depletion for the evolved tholeiitic arc magmas.

Unlike in tholeiitic arc magmas, no synchronous trend of the five proxies mentioned above is observed in calc-alkaline arc magmas. The constant V contents and FeO_T/MnO ratios at $\text{MgO} > 4\text{ wt}\%$ in both average and individual calc-alkaline arcs (Figs. 2 and 3, Figs. S3 and S6) imply that magnetite is not saturated at this early differentiation stage. This is consistent with magnetite being unstable during the early differentiation of hydrous basaltic magmas under $> \sim 1\text{ GPa}$ and redox conditions relevant to arc settings (e.g., between FMQ and FMQ+2, where FMQ is the fayalite-magnetite-quartz oxygen fugacity buffer) (Matjuschkin et al., 2016; Tang et al., 2019b; Sun and Lee, 2022). Accordingly, we suggest that magnetite is not the culprit for the early Fe depletion in calc-alkaline arc magmas, contrary to the traditional perspective that the early Fe depletion in calc-alkaline magmas is due to magnetite fractionation (Osborn, 1959; Sisson and Grove, 1993; Zimmer et al., 2010).

The role of magnetite fractionation for depleting magma Fe contents only becomes important in late-stage differentiation (e.g., $\text{MgO} < 4\text{ wt}\%$). For some calc-alkaline arcs (e.g., Cascades, Central America, and New Zealand), both V contents and FeO_T/MnO start to decrease at $\text{MgO} = \sim 4\text{ wt}\%$ (Figs. S3 and S6), indicative of magnetite saturation at this point. But for some other calc-alkaline arcs (e.g., the Northern Volcanic Zone and the Central Volcanic Zone), the FeO_T/MnO remain constant until the magma MgO contents decrease to $< 2\text{ wt}\%$ and thereupon decreases abruptly (Fig. S6), suggesting that magnetite likely saturates very late for these calc-alkaline arcs with very thick crustal thicknesses. This difference of magnetite saturation timing is consistent with magnetite being suppressed by high pressures, as evidenced by experiments and model calculations (Matjuschkin et al., 2016; Tang et al., 2019b; Sun and Lee, 2022). In both cases, magnetite has no bearing on the early ($\text{MgO} > 4\text{ wt}\%$) Fe depletion in calc-alkaline arc magmas.

4.2. The early Fe enrichment or depletion

In this section, we will focus on the mechanism causing the different Fe trends at the early differentiation stages (at $\text{MgO} > \sim 4\text{ wt}\%$) for both tholeiitic and calc-alkaline arc magmas. Recent studies observed systematic correlations between magma compositions and crustal thickness for global magmatic arcs (Chiaradia, 2014; Farner and Lee, 2017; Chin et al., 2018; Tang et al., 2018). Crustal thickness affects the average pressure of magma storage in the crust, which in turn influences the magma differentiation processes. Indeed, previous experimental investigations showed that different minerals crystallize under different pressures (Fig. 5). Under low pressures (e.g., 0.5 GPa), pyroxenes and olivine are the early fractionating minerals, while under high pressures (e.g., $> 2\text{ GPa}$), garnet and clinopyroxene crystallize initially. The influence of differentiation pressure on magma Fe contents is also supported by the negative correlations between $\text{Fe}_{5.0}/\text{Fe}_{8.0}$ and pressure-sensitive proxies, like La/Yb and Dy/Yb (Fig. 6). Therefore, to understand the mechanism(s) of the different Fe trends, it is necessary to investigate the mineral assemblages fractionated under different pressures.

We will investigate three different pressure conditions for arc magma differentiation to see the early fractionated mineral assemblages. The

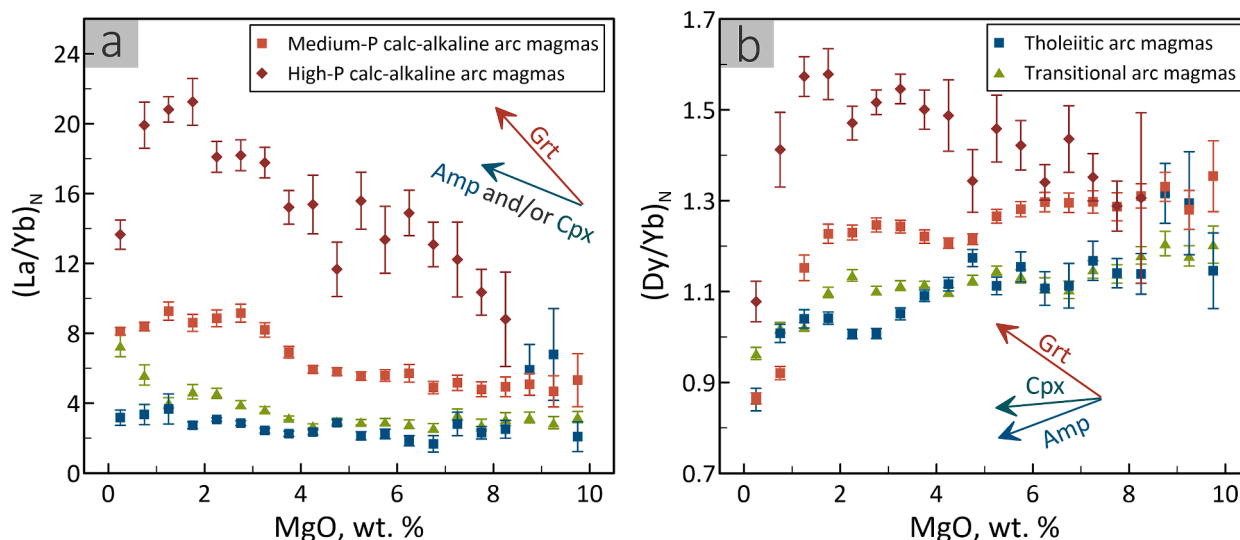


Fig. 4. La/Yb and Dy/Yb differentiation trends in global magmatic arcs. Data sources are provided in the Table S3. Data are binned by 0.5 % MgO content, and within each bin, the mean values of La/Yb and Dy/Yb and the two standard errors are plotted. For each MgO bin, we removed 10% of the samples with the highest values and 10% with the lowest values to alleviate the influence of outliers on the calculation of the averages. $(La/Yb)_N$ and $(Dy/Yb)_N$ denotes CI chondrite normalized values (McDonough and Sun, 1995). The La/Yb and Dy/Yb results for individual arcs are presented in Figs. S4–S6 and results for each group in Fig. S9. Please see Section 4.2 for the explanation of the high- and medium-P calc-alkaline arc magmas. Mineral abbreviations: Amp, amphibole; Cpx, clinopyroxene; Grt, garnet.

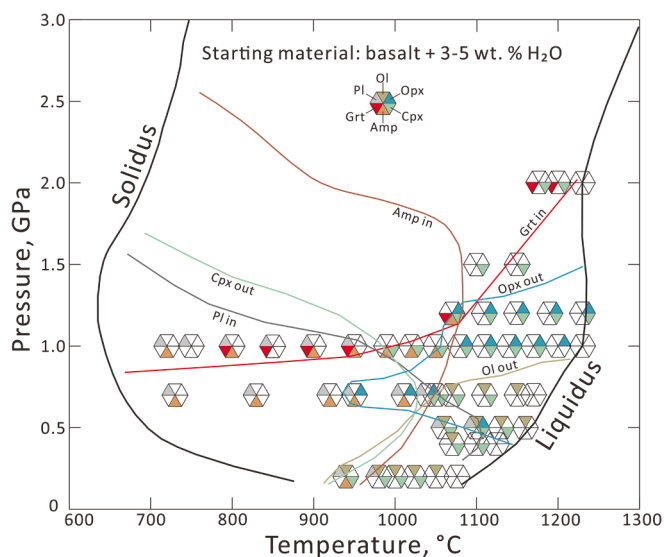


Fig. 5. Pressure–temperature phase diagram for hydrous basaltic magmas. Experimental result sources: > 2 GPa (Green, 1982), 2 GPa and 1.5 GPa (Mercer and Johnston, 2008), 1.2 GPa (Müntener et al., 2001), 1.0 GPa (Ulmer et al., 2018), 0.7 GPa (Nandedkar et al., 2014), 0.5 GPa (Feig et al., 2006), 0.4 GPa (Di Carlo et al., 2006), and 0.2 GPa (Botcharnikov et al., 2008). Solidus is from Green (1982). Minerals: Ol, olivine; Opx, orthopyroxene; Cpx, clinopyroxene; Grt, garnet; Amp, amphibole; Pl, plagioclase.

first one is 0.5–0.8 GPa, which is chosen for the Fe-enriching tholeiitic arcs. This is because tholeiitic arcs have a narrow range of crustal thicknesses of 15–25 km, and thus magmas stalled in the arc roots have differentiation pressures of 0.5–0.8 GPa based on lithostatic pressure. The similar pressure conditions for these tholeiitic arcs are also reflected in the narrow ranges of La/Yb and Dy/Yb, respectively (Fig. S4). Hence, the average La/Yb and Dy/Yb for all the tholeiitic arcs (Fig. 4) are representative for the individual arcs and thus can be directly used to infer mineral fractionation during tholeiitic arc magma differentiation. The other two pressure conditions are chosen for Fe-depleting calc-

alkaline arcs. The Fe-depleting calc-alkaline arcs have a wide range of crustal thicknesses ranging from ~30–40 km to ~65 km, corresponding to Moho pressures ranging from ~1.0–1.3 GPa to ~2.0 GPa. The pressure difference is also revealed in the apparently higher La/Yb and Dy/Yb in thicker continental arcs than those in continental arcs with normal crustal thicknesses (Fig. S6). We here choose the two end member pressure conditions for Fe-depleting calc-alkaline arc magmas: 1.0–1.3 GPa for the ~30–40 km thick calc-alkaline arcs and ~2.0 GPa for the ~65 km thick calc-alkaline arcs. We term these calc-alkaline arc magmas as medium-pressure and high-pressure calc-alkaline arc magmas, respectively. The former is represented by New Zealand, Luzon, Central American, Mexican, and Cascades, and the latter by the Central Volcanic Zone.

4.2.1. Tholeiitic (Fe-enriching) arcs: 0.5–0.8 GPa

It is generally accepted that the early Fe enrichment in mid-ocean ridge magmas, typical of tholeiitic series, is mainly caused by abundant fractionation of plagioclase, a Fe-free mineral (Grove and Baker, 1984). In tholeiitic arcs, however, the initial Fe enrichment is not driven by plagioclase fractionation because the high-water content of primitive arc magmas suppresses plagioclase saturation (Sisson and Grove, 1993; Mercer and Johnston, 2008). For example, during the differentiation of hydrous basaltic magma under 0.7 GPa, plagioclase is not saturated until the temperature drops to ~150–200 °C below the liquidus (Nandedkar et al., 2014). The plagioclase unsaturation at MgO > 4 wt% is also supported by the absence of Eu anomaly (Eu/Eu^* , chondrite-normalized $Eu/\sqrt{(Sm \times Gd)}$) in these magmas (Fig. S7). On the other hand, due to the thin crustal thicknesses for most tholeiitic arcs (< 25 km), magmatic differentiation pressure is low (< 0.8 GPa), which precludes garnet as an early crystallizing phase (Alonso-Perez et al., 2009), consistent with the low Dy/Yb and La/Yb (Fig. 4). Amphibole is also unlikely to fractionate abundantly during hydrous basaltic differentiation under low pressure conditions (Fig. 5), as demonstrated by some experiments that amphibole starts to fractionate until the temperature drops to ~100–150 °C below the liquidus (Di Carlo et al., 2006; Mercer and Johnston, 2008; Nandedkar et al., 2014).

We suggest that the mild Fe enrichment during the early-stage differentiation of tholeiitic arc magmas results from the fractionation of clinopyroxene and olivine. Experiments show that clinopyroxene and

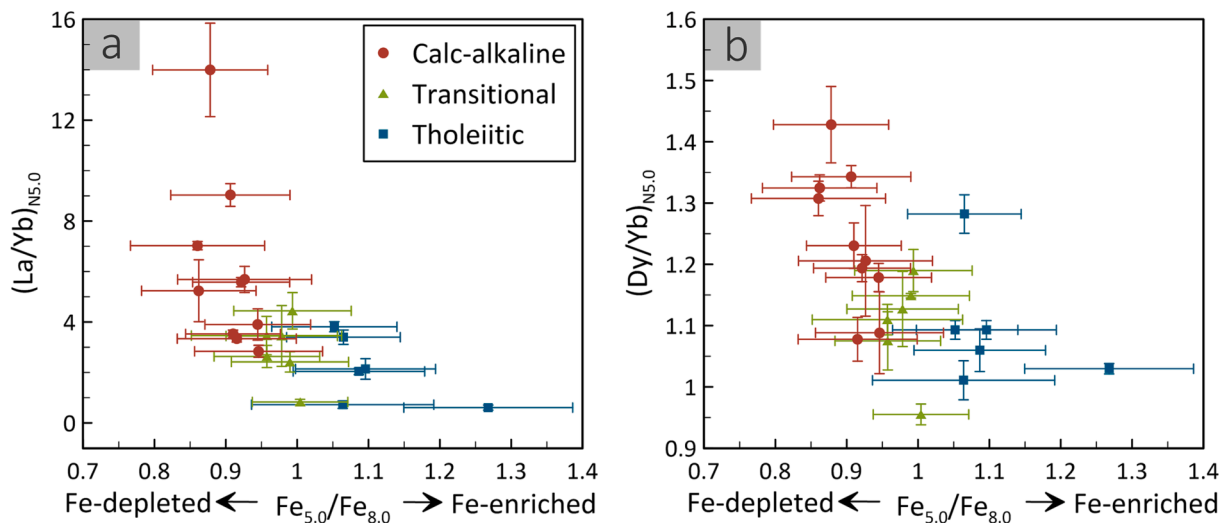


Fig. 6. The relationship between individual arc $Fe_{5.0}/Fe_{8.0}$ and $(La/Yb)_{N5.0}$ (a) and $(Dy/Yb)_{N5.0}$ (b), respectively. Data sources are provided in the Table S2. One dot denotes one individual arc in Table S2. $Fe_{5.0}$ and $Fe_{8.0}$ are the average FeO_T contents for magmas with 4–6 wt% MgO and 7–9 wt% MgO, respectively. To calculate $Fe_{5.0}$, data are binned to 0.5 wt% MgO intervals, and the averages of the four bins is taken as $Fe_{5.0} \pm 2se$ (standard error). $Fe_{8.0} \pm 2se$ is calculated in the same way as $Fe_{5.0} \pm 2se$. $(La/Yb)_N$ and $(Dy/Yb)_N$ denotes CI chondrite (McDonough and Sun, 1995) normalized La/Yb and Dy/Yb. $(La/Yb)_{N5.0}$ and $(Dy/Yb)_{N5.0}$ are calculated in the same way as $Fe_{5.0} \pm 2se$. We emphasize that it is the first-order trend that we try to elucidate in this figure. Given the complexity of natural subduction magmas, it is almost impossible that every single arc would follow a unique pattern. For example, Northeastern Aleutian with a thicker arc crust has lower $(La/Yb)_{N5.0}$ and $(Dy/Yb)_{N5.0}$ than the Western Aleutian with a thinner arc crust. Slab melting contribution has been suggested to be the possible explanation for the high La/Yb in the Western Aleutian (Yogodzinski and Kelemen, 1998). However, slab melting is likely very limited due to the cool thermal structure for the majority of modern subduction zones (Syracuse et al., 2010). The correlations in the figure suggest differentiation pressures exert a first-order control on arc magma Fe depletion degree.

olivine would fractionate as early mineral assemblages during the fractionation of hydrous basaltic magmas under 0.5–0.8 GPa (Di Carlo et al., 2006; Mercer and Johnston, 2008; Nandedkar et al., 2014). Under these conditions, Fe is incompatible in clinopyroxene and slightly compatible in olivine at high temperatures (Nandedkar et al., 2014). Fractionation of both minerals results in a bulk Fe partition coefficient of ~ 0.8 if the initial mineral proportions and Fe partition coefficients for clinopyroxene and olivine from Nandedkar et al. (2014) are used. The dominance of clinopyroxene and olivine fractionation in the early differentiation stages of tholeiitic arc magmas is also consistent with the roughly invariable Sc concentrations at $MgO > 6$ wt% (Fig. S8), as Sc is compatible in clinopyroxene but incompatible in olivine (Lee et al., 2012).

4.2.2. Medium-pressure calc-alkaline (Fe-depleting) arcs: 1.0–1.3 GPa

Experiments show that hydrous basaltic magmas fractionate orthopyroxene and clinopyroxene (\pm olivine and trace spinel) as the high temperature phases at 1.0–1.3 GPa (Baker et al., 1994; Müntener et al., 2001; Grove et al., 2003; Ulmer et al., 2018), corresponding to the Moho pressure conditions of the medium-pressure calc-alkaline arcs (Fig. 5). The early fractionation of orthopyroxene and clinopyroxene is consistent with the slow decline of Sc during differentiation as Sc is slightly incompatible in orthopyroxene and compatible in clinopyroxene (Fig. S8, Lee et al., 2012). When temperature drops to 1000–1100 °C, amphibole starts to fractionate and replaces orthopyroxene at melt MgO content of ~ 3 –4 wt% (Ulmer et al., 2018). Garnet joins amphibole as a liquidus phase at < 1000 °C (Fig. 5). Thus, the early Fe depletion is caused by neither garnet nor amphibole fractionations. This is consistent with the roughly constant La/Yb and Dy/Yb at $Mg > \sim 4$ wt% (Fig. 4). Because Fe is compatible in orthopyroxene and incompatible in clinopyroxene under these P-T conditions, the early Fe depletion in the medium-pressure calc-alkaline arcs is largely caused by orthopyroxene, with a minor role, if any, of spinel (Müntener et al., 2001; Ulmer et al., 2018).

4.2.3. High-pressure calc-alkaline (Fe-depleting) arcs: 2.0 GPa

At ~ 2 GPa, garnet and clinopyroxene are the high temperature

liquidus phases during the differentiation of hydrous basaltic magmas (Fig. 5, Green, 1982; Mercer and Johnston, 2008). Arc magma differentiation at this pressure produces garnet-pyroxenites as a major type of cumulate over a large temperature range. Garnet-pyroxenites have been observed as xenoliths in the Sierra Nevada (Lee et al., 2006) and Arizona (Erdman et al., 2016; Chen et al., 2020). The early fractionation of garnet is also reflected in the increasing La/Yb and Dy/Yb with decreasing MgO at $MgO > 4$ wt% (Fig. 4). Because both garnet and clinopyroxene are compatible with Sc (Lee et al., 2012), their fractionation would cause Sc to decrease in melts (Fig. S8). Thus, magma Fe is scavenged principally by garnet during this stage. When the temperature drops to 1000–1100 °C, amphibole saturates and joins garnet and clinopyroxene in the fractionation assemblage (Fig. 5). From this point, the combined fractionation of garnet and amphibole continues to lower the magma Fe contents. It is still not clear if amphibole is fractionated at $MgO > 4$ wt% when the pressure is ≥ 2 GPa due to the limited experimental data for high-pressure hydrous basalt fractionation. As shown in Fig. 5, as the pressure increases from ~ 1.0 to ~ 2.0 GPa, the temperature for garnet occurrence increases gradually, suggesting that garnet plays a more dominant role for the early Fe depletion as calc-alkaline arcs thicken.

4.3. The role of high-pressure differentiation in continental crust formation

We have used some geochemical proxies to reveal the petrological mechanisms causing the initial Fe enrichment in tholeiitic oceanic arcs and the initial Fe depletion in calc-alkaline continental arcs. The increasing of FeO_T , TiO_2 , MnO, and V contents and constant FeO_T/MnO during differentiation at $MgO > 4$ –5 wt% support that magnetite stays unstable at the early differentiation stages in both tholeiitic and calc-alkaline arcs and thus has no bearing on the early Fe depletion in calc-alkaline arc magmas. This is contrary to the popular model that magnetite is the culprit for the early Fe depletion in calc-alkaline arc magmas (Osborn, 1959; Sisson and Grove, 1993; Botcharnikov et al., 2008; Hamada and Fujii, 2008; Zimmer et al., 2010; Chin et al., 2018). Experimental work (Nandedkar et al., 2014; Matjuschkin et al., 2016)

and thermodynamic modeling (Tang et al., 2019b) are also against early magnetite fractionation during arc magma differentiation at high pressures. Then, we combine the differentiation trends of La/Yb, Dy/Yb, and Sc and reported experimental results to demonstrate that the early Fe enrichment in tholeiitic arcs is caused by the fractionation of clinopyroxene and olivine. And the early Fe depletion in calc-alkaline arcs is produced by garnet fractionation under high-pressure conditions and by orthopyroxene under medium-pressure conditions.

Our results also have important implications for the roles of different arc settings in the growth of the Phanerozoic continental crust. The average composition of the Phanerozoic continental crust shows a clear resemblance to those of the calc-alkaline magmas in continental arcs but differs from the tholeiitic oceanic arc magmas and the transitional arc magmas significantly. Oceanic arc magmas and the transitional arc

magmas have too high FeO_T, MnO, and V contents (and probably TiO₂) to match the composition of the continental crust (Fig. 2). By contrast, continental arc magmas show similar FeO_T, MnO, and V contents (and probably TiO₂) to the average continental crust (Fig. 2). Furthermore, we compare La/Yb and Dy/Yb, FeO_T/MnO in the average upper continental crust with those in the evolved arc magmas with MgO ≤ 4 wt% (Figs. 7 and 8). The results show that the upper continental crust has apparently higher La/Yb, Dy/Yb, and FeO_T/MnO than those of the evolved magmas from tholeiitic and transitional arcs but falls within the interval between the evolved magmas from the medium-pressure and high-pressure calc-alkaline arcs. Furthermore, it seems that medium-pressure arc magmas alone cannot account for the high La/Yb and FeO_T/MnO in the upper continental crust.

Implicit in this compositional similarity between the upper

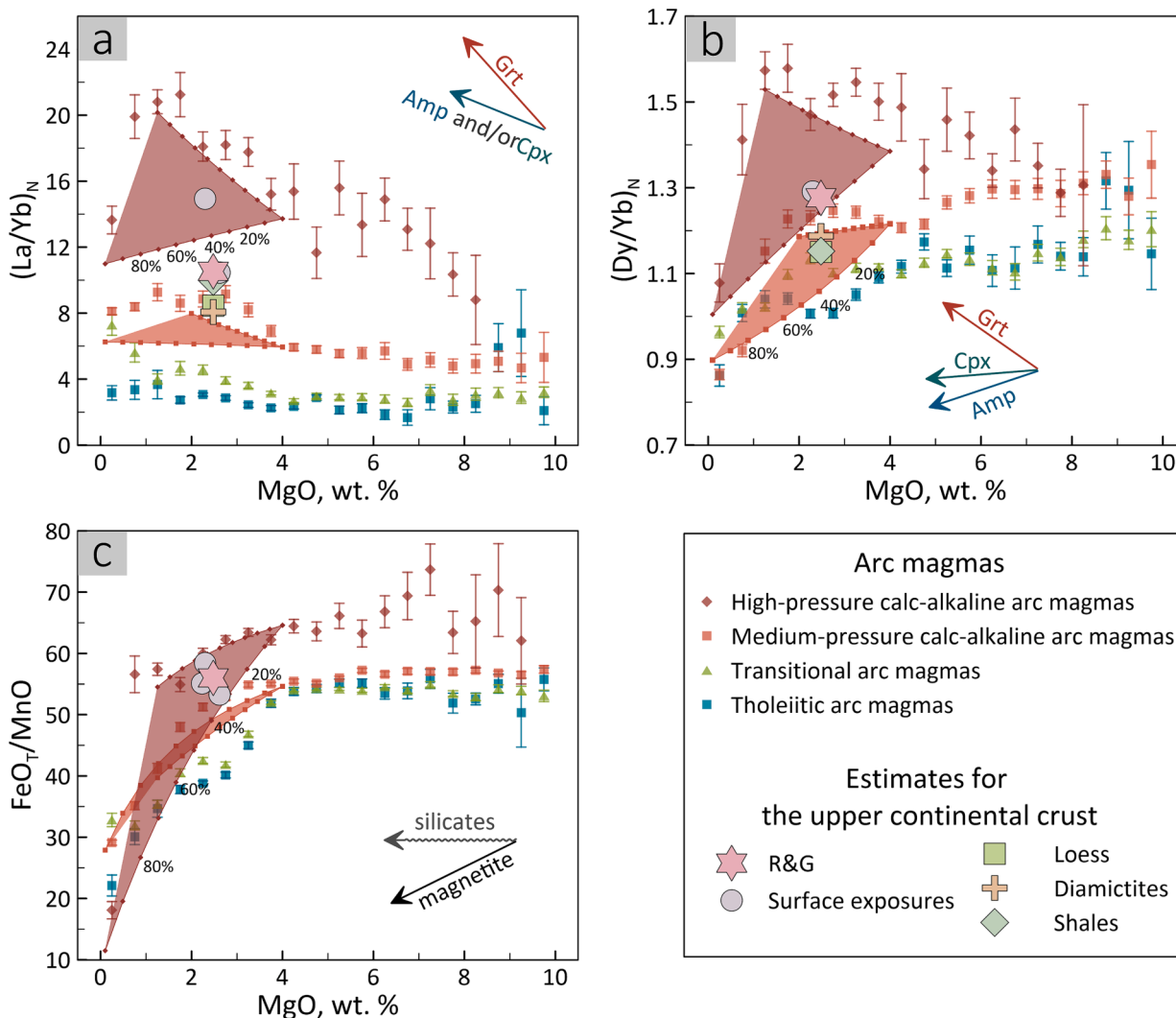


Fig. 7. Comparison of the La/Yb, Dy/Yb, and FeO_T/MnO systematics in between evolved arc magmas (MgO ≤ 4 wt%) and the average upper continental crust (UCC). The high-pressure and medium pressure calc-alkaline arc magmas are two end members of the calc-alkaline arc magmas with various differentiation pressures. The former is represented by the Central Volcanic Zone with crustal thickness of ~65 km and the latter by New Zealand, Luzon, Central American, Mexican, and Cascades with crustal thicknesses ranging from ~30 to 40 km. R&G is the estimate for the average UCC from Rudnick and Gao (2003). Data for surface exposures are UCC estimates based on large area surface sampling method reported by Shaw et al. (1967, 1976), Fahrig and Eade (1968), and Gao et al. (1998). Loess and post-Archean shales and diamictites are widely thought to be able to represent the average insoluble element composition in the Phanerozoic UCC. Average loess La/Yb and Dy/Yb are from the literature (Gallet et al., 1996, 1998; Barth et al., 2000; Jahn et al., 2001; Park et al., 2012; Chauvel et al., 2014). Average La/Yb and Dy/Yb for post-Archean shales are from Barth et al. (2000) and for post-Archean diamictites from Gaschnig et al. (2016). Because Mg is highly soluble, its abundance in the UCC cannot be directly obtained from sedimentary rocks/sediments. We thus use R&G MgO estimate for the UCC for plotting loess, shales, and diamictites. Shaded areas show the mixing fields between magmas with MgO = 3.9–4.1 wt% with more evolved magmas in the high-pressure and medium-pressure calc-alkaline arcs, respectively. For high-pressure calc-alkaline arcs, we used samples with 0–0.2 wt% and 1.0–1.5 wt% MgO as the more evolved endmembers; for medium-pressure calc-alkaline arcs, we used samples with 0–0.2 wt% and 1.9–2.1 wt% MgO as the more evolved endmembers. The endmember mixing curves are marked at 10% mixing intervals. The calculations show that high-pressure calc-alkaline arc magmas are an essential component for the average upper continental crust.

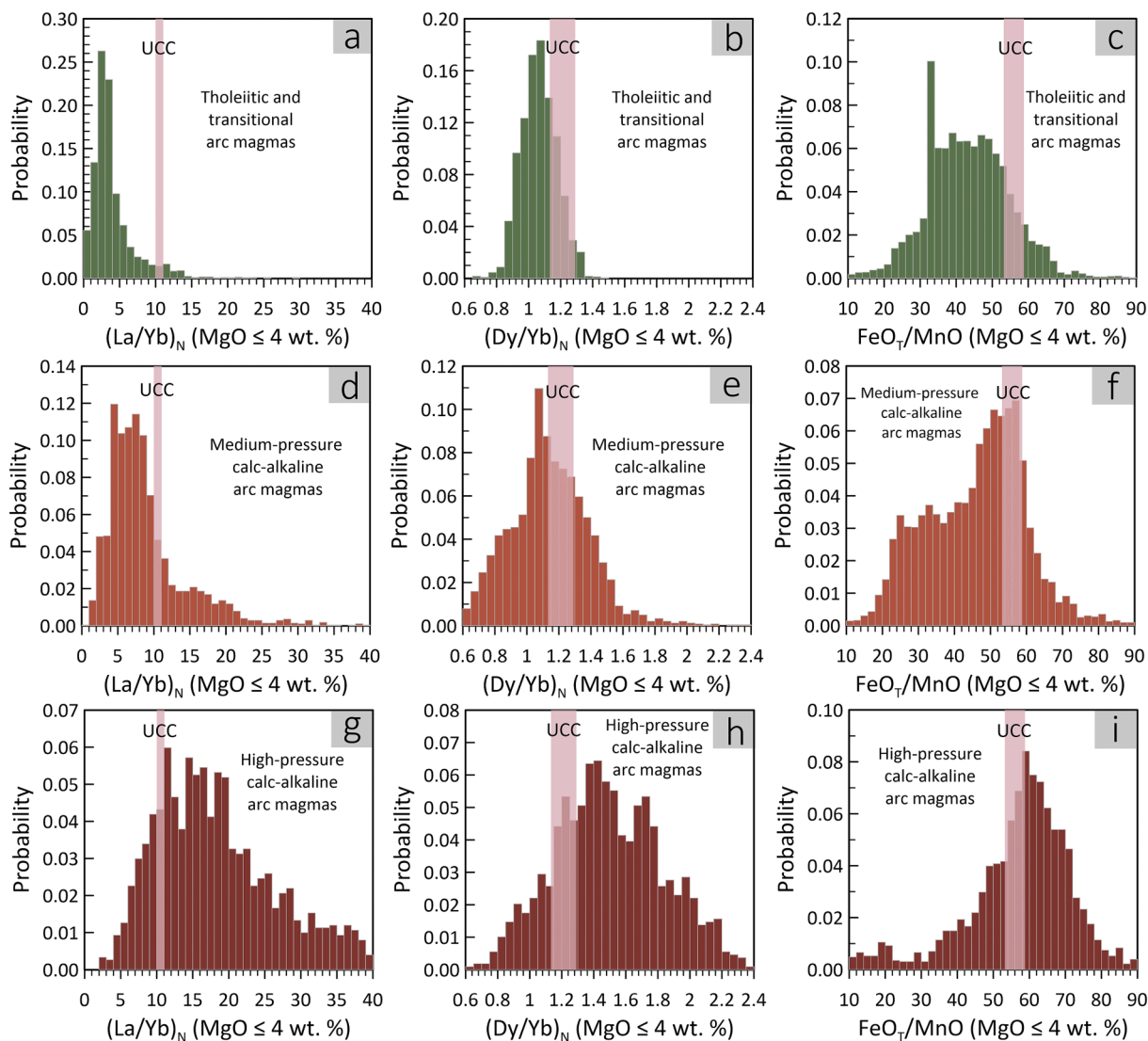


Fig. 8. Comparison of the La/Yb (a, d, g), Dy/Yb (b, e, h), and FeO₇/MnO (c, f, i) systematics in between evolved arc magmas (MgO ≤ 4 wt%) and the average upper continental crust (UCC). a, b, and c, tholeiitic and transitional arc magmas; d, e and f, medium-pressure calc-alkaline arc magmas; g, h, and i, high-pressure calc-alkaline arc magmas. The high-pressure and medium pressure calc-alkaline arc magmas are two end members of the calc-alkaline arc magmas with various differentiation pressures. The former are represented by magmas from the Central Volcanic Zone with crustal thickness of ~65 km and the latter by magmas from New Zealand, Luzon, Central American, Mexican, and Cascades with crustal thicknesses ranging from ~30 to 40 km. The UCC estimates are from Rudnick and Gao (2003).

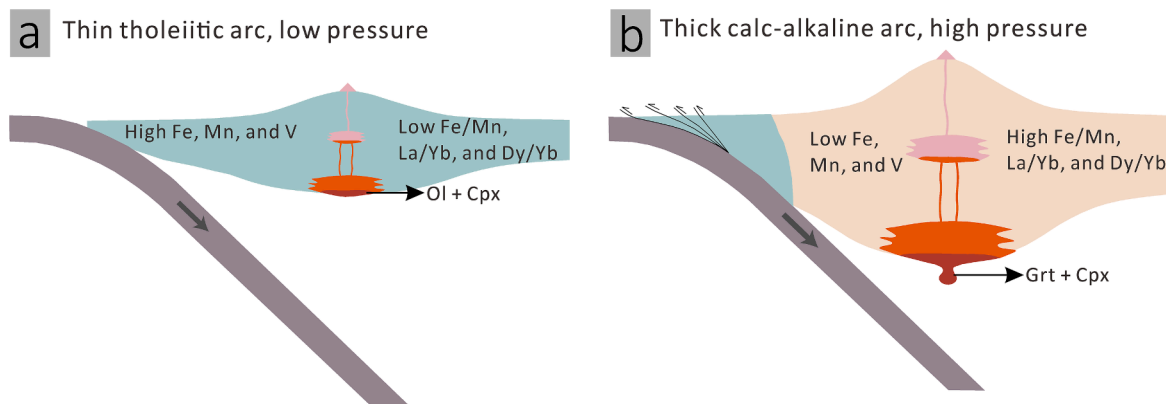


Fig. 9. Cartoons for magma differentiation in a thin tholeiitic arc (a) and a thick calc-alkaline arc (b) and the compositions of the produced arc crusts.

continental crust and the calc-alkaline arcs, which have thicker crusts than tholeiitic arcs, is that high-pressure differentiation is an inherent nature of the Phanerozoic continental crust. This inference sheds additional light on the debate that whether deep or shallow differentiation is a crucial process for the formation of the continental crust. Some researchers argue that mid- to upper-crustal level differentiation dominates the production of intermediate arc magmas and, by that, the continental crust (Blatter et al., 2013; Adam et al., 2016), while others suggest high-pressure differentiation in the lower crust or at the crust-mantle boundary exerts a first-order control on arc magma composition and the formation of the continental crust (Annen et al., 2006; Alonso-Perez et al., 2009; Chapman et al., 2016; Farner and Lee, 2017; Müntener and Ulmer, 2018; Tang et al., 2019a). Our results here show that lateral accretion of island (or tholeiitic) and transitional arcs alone cannot produce the garnet fractionation signature in the upper continental crust (Fig. 9a). Island arcs may eventually accrete onto an old continental margin due to subduction and trench migration (Busby, 2004). As the subduction continues, new mantle-derived melts underplate the accreted terrane, and then a continental arc is produced (Fig. 9b, Lee et al., 2007). The crust of this continental arc thickens as new magmas are further added into the arc setting. The thick arc crust allows the underplated magmas differentiate at relatively high pressures, resulting in calc-alkaline magma series (Fig. 9b). We argue that the Phanerozoic continental crust grows mainly through this type of vertical accretion of calc-alkaline arc magmas in a thickened crust. Under this high-pressure condition, probably at the crust-mantle boundary with the crust acting as a density filter (Green, 1982), mantle-derived magmas are transformed into arc crust having a similar composition to the Phanerozoic continental crust. This implication is also consistent with the studies of Cu concentrations (Chiaradia, 2014; Chen et al., 2020), Nb/Ta ratios (Tang et al., 2019a), Fe isotopes (Du et al., 2022), and Mg# (molar ratio of Mg/(Mg + Fe_T)) (Tang et al., 2023) in arc magmas, which show that the low Cu concentrations, low Nb/Ta, heavy Fe isotopic composition, and high Mg# in the continental crust are largely produced in thick continental arcs.

It is worth noting that, although active arcs with >60 km crustal thickness are currently not common (represented by the Central Volcanic Zone), they may be extensively distributed in Earth's history. Examples include Sierra Nevada, Kohistan, Gangdese, Coast Mountains, and northern Mexican Cordillera (Jagoutz and Schmidt, 2013; Profeta et al., 2015; Zhu et al., 2017; Chapman et al., 2020). These high-pressure calc-alkaline arcs are thicker than the preserved thickness of the Phanerozoic continental crust (~35 km, Huang et al., 2013), suggesting that the lower parts of the thick calc-alkaline arcs have been removed and may have sunk back into the mantle through density sorting (Ringwood and Green, 1966; Herzberg et al., 1983; Arndt and Goldstein, 1989; Kay and Kay, 1991; Ducea and Saleeby, 1996). The removal of the high-density and mafic lower crust is also a popular solution for the "crust compositional paradox" (Rudnick, 1995; Jagoutz and Behn, 2013; Lee, 2014).

5. Conclusions

- (1) Tholeiitic arc magmas differentiate under relatively low pressures (e.g., ≤ 0.8 GPa). The early Fe enrichment is mainly caused by clinopyroxene fractionation, and the late-stage Fe depletion results from the fractionation of magnetite and, to a lesser extent, amphibole. The coherent trends of the contents of FeO_T, TiO₂, MnO, and V and the FeO_T/MnO ratio provide strong evidence for the start of magnetite fractionation at MgO = ~4–5 wt% in tholeiitic arc magmas. This coherency, in turn, demonstrates the reliability of using FeO_T/MnO to track magnetite fractionation.
- (2) Calc-alkaline arc magmas differentiate under relatively high pressures (e.g., ≥ 1 GPa). Magnetite has no bearing on the early Fe depletion for all calc-alkaline arc magmas and its contribution for Fe depletion only becomes remarkable in late-stage

differentiation (MgO < 4 wt%). The early (MgO > 4 wt%) Fe depletion is mainly caused by orthopyroxene fractionation for medium-pressure (1.0–1.3 GPa) calc-alkaline arc magmas and by garnet (\pm amphibole) fractionation for high-pressure ones (≥ 2 GPa). As magma differentiation pressures increase, the role of garnet fractionation played in reducing magma Fe contents becomes more prominent.

- (3) The evolved magmas (MgO ≤ 4 wt%) from tholeiitic and transitional arcs have too low La/Yb, Dy/Yb, and FeO_T/MnO compared to the average upper continental crust. By contrast, the evolved magmas from calc-alkaline arcs show similar La/Yb, Dy/Yb, and FeO_T/MnO to the average upper continental crust, suggesting that calc-alkaline arc magmas are an essential component for the continental crust. The comparisons show that the upper continental crust has an intrinsic feature of garnet fractionation. We thus conclude that high-pressure differentiation is a necessary step for making the Phanerozoic continental crust.

Declaration of Competing Interest

The authors declare that they have no known competing financial interests or personal relationships that could have appeared to influence the work reported in this paper.

Acknowledgements

This work was supported by the National Natural Science Foundation of China (42073024), the Natural Science Foundation of Hubei Province (2020CFA045), and the State Key Laboratory of Geological Processes and Mineral Resources (MSFGPMR2022-1). We thank Roberta Rudnick and WJ Collins for comments on an earlier version of the manuscript. We thank Emily Chin and an anonymous reviewer for their constructive reviews and Adam Simon and Jeffrey Catalano for the editorial handling and insightful comments.

Appendix A. Supplementary material

The geochemical data for individual arcs are presented in Figures S1–S6, the europium anomalies for tholeiitic arcs in Figure S7, the scandium differentiation trends in Figure S8, and La/Yb and Dy/Yb data for each arc magma sample in Figure S9. All these figures can be found in the supplementary data 1 file. Compiled data for partition coefficients of La, Dy, and Yb between minerals and silicate magmas are presented in Table S1 (supplementary data 2 file). Detailed information for the 22 magmatic arcs is presented in Table S2 (supplementary data 3 file). Compiled data for arc magma compositions are presented in Table S3 (supplementary data 4 file). All these tables and figures can be found online. Supplementary material to this article can be found online at <https://doi.org/10.1016/j.gca.2023.07.002>.

References

- Adam, J., Turner, S., Rushmer, T., 2016. The genesis of silicic arc magmas in shallow crustal cold zones. *Lithos* 264, 472–494.
- Alonso-Perez, R., Müntener, O., Ulmer, P., 2009. Igneous garnet and amphibole fractionation in the roots of island arcs: experimental constraints on andesitic liquids. *Contrib. Mineral. Petrol.* 157 (4), 541–558.
- Annen, C., Blundy, J.D., Sparks, R.S.J., 2006. The genesis of intermediate and silicic magmas in deep crustal hot zones. *J. Petrol.* 47 (3), 505–539.
- Arndt, N.T., Goldstein, S.L., 1989. An open boundary between lower continental crust and mantle: its role in crust formation and crustal recycling. *Tectonophysics* 161 (3–4), 201–212.
- Baker, M.B., Grove, T.L., Price, R., 1994. Primitive basalts and andesites from the Mt. Shasta region, N. California: products of varying melt fraction and water content. *Contrib. Mineral. Petrol.* 118 (2), 111–129.
- Barber, N.D., Edmonds, M., Jenner, F., Audétat, A., Williams, H., 2021. Amphibole control on copper systematics in arcs: Insights from the analysis of global datasets. *Geochim. Cosmochim. Acta* 307, 192–211.
- Barth, M.G., McDonough, W.F., Rudnick, R.L., 2000. Tracking the budget of Nb and Ta in the continental crust. *Chem. Geol.* 165 (3–4), 197–213.

- Blatter, D.L., Sisson, T.W., Ben Hankins, W., 2013. Crystallization of oxidized, moderately hydrous arc basalt at mid- to lower-crustal pressures: implications for andesite genesis. *Contrib. Mineral. Petrol.* 166 (3), 861–886.
- Botcharnikov, R.E., Almeev, R.R., Koepke, J., Holtz, F., 2008. Phase Relations and liquid lines of descent in hydrous ferrobasalt—implications for the Skaergaard intrusion and Columbia river flood basalts. *J. Petrol.* 49 (9), 1687–1727.
- Busby, C., 2004. Continental growth at convergent margins facing large ocean basins: a case study from Mesozoic convergent-margin basins of Baja California. Mexico. *Tectonophysics* 392 (1), 241–277.
- Cawthorn, R.G., O'Hara, M.J., 1976. Amphibole fractionation in calc-alkaline magma genesis. *Am. J. Sci.* 276 (3), 309–329.
- Chapman, T., Clarke, G.L., Daczko, N.R., 2016. Crustal differentiation in a thickened arc—evaluating depth dependences. *J. Petrol.* 57 (3), 595–620.
- Chapman, J.B., Greig, R., Haxel, G.B., 2020. Geochemical evidence for an orogenic plateau in the southern U.S. and northern Mexican Cordillera during the Laramide orogeny. *Geology* 48 (2), 164–168.
- Chauvel, C., Garçon, M., Bureau, S., Besnault, A., Jahn, B.-M., Ding, Z., 2014. Constraints from loess on the Hf–Nd isotopic composition of the upper continental crust. *Earth Planet. Sci. Lett.* 388, 48–58.
- Chen, K., Tang, M., Lee, C.-T.-A., Wang, Z., Zou, Z., Hu, Z., Liu, Y., 2020. Sulfide-bearing cumulates in deep continental arcs: The missing copper reservoir. *Earth Planet. Sci. Lett.* 531, 115971.
- Chiaradia, M., 2014. Copper enrichment in arc magmas controlled by overriding plate thickness. *Nature Geosci.* 7 (1), 43–46.
- Chin, E.J., Shimizu, K., Bybee, G.M., Erdman, M.E., 2018. On the development of the calc-alkaline and tholeiitic magma series: A deep crustal cumulate perspective. *Earth Planet. Sci. Lett.* 482, 277–287.
- Davidson, J., Turner, S., Handley, H., Macpherson, C., Dosseto, A., 2007. Amphibole “sponge” in arc crust? *Geology* 35 (9), 787–790.
- Di Carlo, I.D.A., Pichavant, M., Rotolo, S.G., Scaillet, B., 2006. Experimental crystallization of a high-K arc basalt: the golden pumice, Stromboli Volcano (Italy). *J. Petrol.* 47 (7), 1317–1343.
- Du, D.-H., Tang, M., Li, W., Kay, S.M., Wang, X.-L., 2022. What drives Fe depletion in calc-alkaline magma differentiation: Insights from Fe isotopes. *Geology* 50 (5), 552–556.
- Ducea, M.N., Saleeby, J.B., 1996. Buoyancy sources for a large, unrooted mountain range, the Sierra Nevada, California: Evidence from xenolith thermobarometry. *J. Geophys. Res.: Solid Earth* 101 (B4), 8229–8244.
- Erdman, M.E., Lee, C.-T.-A., Levander, A., Jiang, H., 2016. Role of arc magmatism and lower crustal foundering in controlling elevation history of the Nevada-plano and Colorado Plateau: A case study of pyroxenitic lower crust from central Arizona, USA. *Earth Planet. Sci. Lett.* 439, 48–57.
- Fahrig, W.F., Eade, K.E., 1968. The chemical evolution of the Canadian Shield. *Can. J. Earth Sci.* 5 (5), 1247–1252.
- Farner, M.J., Lee, C.-T.-A., 2017. Effects of crustal thickness on magmatic differentiation in subduction zone volcanism: A global study. *Earth Planet. Sci. Lett.* 470, 96–107.
- Feig, S.T., Koepke, J., Snow, J.E., 2006. Effect of water on tholeiitic basalt phase equilibria: an experimental study under oxidizing conditions. *Contrib. Mineral. Petrol.* 152 (5), 611–638.
- Gallet, S., Jahn, B.-M., Torii, M., 1996. Geochemical characterization of the Luochuan loess-paleosol sequence, China, and paleoclimatic implications. *Chem. Geol.* 133 (1–4), 67–88.
- Gallet, S., Jahn, B.-M., Van Vliet Lanoë, B., Dia, A., Rossello, E., 1998. Loess geochemistry and its implications for particle origin and composition of the upper continental crust. *Earth Planet. Sci. Lett.* 156 (3–4), 157–172.
- Gao, S., Luo, T.C., Zhang, B.R., Zhang, H.F., Han, Y.W., Zhao, Z.D., Hu, Y.K., 1998. Chemical composition of the continental crust as revealed by studies in East China. *Geochim. Cosmochim. Acta* 62 (11), 1959–1975.
- Gaschnig, R.M., Rudnick, R.L., McDonough, W.F., Kaufman, A.J., Valley, J.W., Hu, Z., Gao, S., Beck, M.L., 2016. Compositional evolution of the upper continental crust through time, as constrained by ancient glacial diamicites. *Geochim. Cosmochim. Acta* 186, 316–343.
- Green, T.H., 1982. Anatectic of mafic crust and high pressure crystallization of andesite. In: Thorpe, R.S. (Ed.), *Andesites: Orogenic andesites and Related Rocks*. John Wiley & Sons, New York.
- Green, T.H., Ringwood, A.E., 1967. Crystallization of basalt and andesite under high pressure hydrous conditions. *Earth Planet. Sci. Lett.* 3, 481–489.
- Green, T.H., Ringwood, A.E., 1968a. Genesis of the calc-alkaline igneous rock suite. *Contrib. Mineral. Petrol.* 18 (2), 105–162.
- Green, T.H., Ringwood, A.E., 1968b. Origin of garnet phenocrysts in calc-alkaline rocks. *Contrib. Mineral. Petrol.* 18 (2), 163–174.
- Grove, T.L., Baker, M.B., 1984. Phase equilibrium controls on the tholeiitic versus calc-alkaline differentiation trends. *J. Geophys. Res.: Solid Earth* 89 (B5), 3253–3274.
- Grove, T.L., Brown, S.M., 2018. Magmatic processes leading to compositional diversity in igneous rocks: Bowen (1928) revisited. *Am. J. Sci.* 318 (1), 1–28.
- Grove, T.L., Elkins-Tanton, L.T., Parman, S.W., Chatterjee, N., Müntener, O., Gaetani, G. A., 2003. Fractional crystallization and mantle-melting controls on calc-alkaline differentiation trends. *Contrib. Mineral. Petrol.* 145 (5), 515–533.
- Hamada, M., Fujii, T., 2008. Experimental constraints on the effects of pressure and H₂O on the fractional crystallization of high-Mg island arc basalt. *Contrib. Mineral. Petrol.* 155 (6), 767–790.
- Herzberg, C.T., Fyfe, W.S., Carr, M.J., 1983. Density constraints on the formation of the continental Moho and crust. *Contrib. Mineral. Petrol.* 84 (1), 1–5.
- Huang, Y., Chubakov, V., Mantovani, F., Rudnick, R.L., McDonough, W.F., 2013. A reference Earth model for the heat producing elements and associated geoneutrino flux. *Geochim. Geophys. Geosyst.* 2003–2029.
- Huang, W.-L., Wyllie, P.J., 1986. Phase relationships of gabbro-tonalite-granite-water at 15 kbar with applications to differentiation and anatexis. *Am. Mineral.* 71 (3–4), 301–316.
- Irvine, T.N., Baragar, W.R.A., 1971. A Guide to the Chemical Classification of the Common Volcanic Rocks. *Can. J. Earth Sci.* 8 (5), 523–548.
- Jagoutz, O., Behn, M.D., 2013. Foundering of lower island-arc crust as an explanation for the origin of the continental Moho. *Nature* 504 (7478), 131–134.
- Jagoutz, O., Schmidt, M.W., 2013. The composition of the foundered complement to the continental crust and a re-evaluation of fluxes in arcs. *Earth Planet. Sci. Lett.* 371–372, 177–190.
- Jahn, B.-M., Gallet, S., Han, J., 2001. Geochemistry of the Xining, Xifeng and Jixian sections, Loess Plateau of China: eolian dust provenance and paleosol evolution during the last 140 ka. *Chem. Geol.* 178 (1–4), 71–94.
- Kay, R.W., Kay, S.M., 1991. Creation and destruction of lower continental crust. *Geol. Rundsch.* 80 (2), 259–278.
- Keller, C.B., Schoene, B., Barboni, M., Samperton, K.M., Husson, J.M., 2015. Volcanic-plutonic parity and the differentiation of the continental crust. *Nature* 523 (7560), 301–307.
- Larocque, J., Canil, D., 2010. The role of amphibole in the evolution of arc magmas and crust: the case from the Jurassic Bonanza arc section, Vancouver Island, Canada. *Contrib. Mineral. Petrol.* 159 (4), 475–492.
- Lee, C.-T.-A., 2014. 4.12 - Physics and chemistry of deep continental crust recycling. In: Holland, H.D., Turekian, K.K. (Eds.), *Treatise on Geochemistry*, second ed. Elsevier, Oxford, pp. 423–456.
- Lee, C.-T.-A., Cheng, X., Horodyskyj, U., 2006. The development and refinement of continental arcs by primary basaltic magmatism, garnet pyroxenite accumulation, basaltic recharge and delamination: insights from the Sierra Nevada, California. *Contrib. Mineral. Petrol.* 151 (2), 222–242.
- Lee, C.-T.-A., Morton, D.M., Kistler, R.W., Baird, A.K., 2007. Petrology and tectonics of Phanerozoic continent formation: From island arcs to accretion and continental arc magmatism. *Earth Planet. Sci. Lett.* 263 (3–4), 370–387.
- Lee, C.-T.-A., Luffi, P., Chin, E.J., Bouchet, R., Dasgupta, R., Morton, D.M., Le Roux, V., Yin, Q.-Z., Jin, D., 2012. Copper systematics in arc magmas and implications for crust-mantle differentiation. *Science* 336 (6077), 64–68.
- Matjuschkin, V., Blundy, J.D., Brooker, R.A., 2016. The effect of pressure on sulphur speciation in mid- to deep-crustal arc magmas and implications for the formation of porphyry copper deposits. *Contrib. Mineral. Petrol.* 171 (7), 66.
- McDonough, W.F., Sun, S.S., 1995. The composition of the Earth. *Chem. Geol.* 120 (3–4), 223–253.
- Mercer, C.N., Johnston, A.D., 2008. Experimental studies of the P–T–H₂O near-liquidus phase relations of basaltic andesite from North Sister Volcano, High Oregon Cascades: constraints on lower-crustal mineral assemblages. *Contrib. Mineral. Petrol.* 155 (5), 571–592.
- Miyashiro, A., 1974. Volcanic rock series in island arcs and active continental margins. *Am. J. Sci.* 274 (4), 321–355.
- Müntener, O., Kelemen, P.B., Grove, T.L., 2001. The role of H₂O during crystallization of primitive arc magmas under uppermost mantle conditions and genesis of igneous pyroxenites: an experimental study. *Contrib. Mineral. Petrol.* 141 (6), 643–658.
- Müntener, O., Ulmer, P., 2018. Arc crust formation and differentiation constrained by experimental petrology. *Am. J. Sci.* 318 (1), 64–89.
- Nandedkar, R.H., Ulmer, P., Müntener, O., 2014. Fractional crystallization of primitive, hydrous arc magmas: an experimental study at 0.7 GPa. *Contrib. Mineral. Petrol.* 167 (6), 1015.
- Osborn, E.F., 1959. Role of oxygen pressure in the crystallization and differentiation of basaltic magma. *Am. J. Sci.* 257 (9), 609–647.
- Park, J.-W., Hu, Z., Gao, S., Campbell, I.H., Gong, H., 2012. Platinum group element abundances in the upper continental crust revisited—New constraints from analyses of Chinese loess. *Geochim. Cosmochim. Acta* 93, 63–76.
- Profeta, L., Ducea, M.N., Chapman, J.B., Paterson, S.R., Gonzales, S.M.H., Kirsch, M., Petrescu, L., DeCelles, P.G., 2015. Quantifying crustal thickness over time in magmatic arcs. *Sci. Rep.* 5, 17786.
- Ringwood, A.E., Green, D.H., 1966. An experimental investigation of the Gabbro-Eclogite transformation and some geophysical implications. *Tectonophysics* 3 (5), 383–427.
- Rudnick, R.L., 1995. Making continental crust. *Nature* 378 (6557), 571–578.
- Rudnick, R.L., Gao, S., 2003. 3.01 - Composition of the continental crust. In: Holland, H. D., Turekian, K.K. (Eds.), *Treatise on Geochemistry*, 1st ed. Pergamon, Oxford, pp. 1–64.
- Rudnick, R.L., Taylor, S.R., 1986. Geochemical constraints on the origin of Archaean tonalitic-trondhjemitic rocks and implications for lower crustal composition. *Geol. Soc. London Spec. Publ.* 24 (1), 179–191.
- Shaw, D.M., Reilly, G.A., Muysson, J.R., Pattenden, G.E., Campbell, F.E., 1967. An estimate of the chemical composition of the Canadian Precambrian Shield. *Can. J. Earth Sci.* 4 (5), 829–853.
- Shaw, D.M., Dostal, J., Keays, R.R., 1976. Additional estimates of continental surface Precambrian shield composition in Canada. *Geochim. Cosmochim. Acta* 40 (1), 73–83.
- Sisson, T.W., Grove, T.L., 1993. Experimental investigations of the role of H₂O in calc-alkaline differentiation and subduction zone magmatism. *Contrib. Mineral. Petrol.* 113 (2), 143–166.
- Sun, C., Lee, C.-T.-A., 2022. Redox evolution of crystallizing magmas with C–H–O–S volatiles and its implications for atmospheric oxygenation. *Geochim. Cosmochim. Acta* 338, 302–321.
- Syracuse, E.M., van Keken, P.E., Abers, G.A., 2010. The global range of subduction zone thermal models. *Phys. Earth Planet. In.* 183 (1), 73–90.
- Tang, M., Erdman, M., Eldridge, G., Lee, C.-T.-A., 2018. The redox “filter” beneath magmatic orogens and the formation of continental crust. *Sci. Adv.* 4 (5).

- Tang, M., Lee, C.-T.-A., Chen, K., Erdman, M., Costin, G., Jiang, H., 2019a. Nb/Ta systematics in arc magma differentiation and the role of arclogites in continent formation. *Nat. Commun.* 10 (1), 235.
- Tang, M., Lee, C.-T.-A., Costin, G., Höfer, H.E., 2019b. Recycling reduced iron at the base of magmatic orogens. *Earth Planet. Sci. Lett.* 528, 115827.
- Tang, M., Lee, C.-T.A., Rudnick, R.L., Condie, K.C., 2020. Rapid mantle convection drove massive crustal thickening in the late Archean. *Geochim. Cosmochim. Acta* 278, 6–15.
- Tang, M., Liu, X., Chen, K., 2023. High Mg# of the continental crust explained by calc-alkaline differentiation. *Natl. Sci. Rev.* 10 (3), nwac258.
- Taylor, S.R., 1977. Island arc models and the composition of the continental crust. In: Talwani, M., Pitman, W.C. (Eds.), *Island Arcs, Deep Sea Trenches and Back-Arc Basins*.
- Taylor, S.R., White, A.J.R., 1965. Geochemistry of andesites and the growth of continents. *Nature* 208, 271.
- Toplis, M.J., Corgne, A., 2002. An experimental study of element partitioning between magnetite, clinopyroxene and iron-bearing silicate liquids with particular emphasis on vanadium. *Contrib. Mineral. Petrol.* 144 (1), 22–37.
- Ulmer, P., Kaegi, R., Müntener, O., 2018. Experimentally derived intermediate to silica-rich arc magmas by fractional and equilibrium crystallization at 1.0 GPa: an evaluation of phase relationships, compositions, liquid lines of descent and oxygen fugacity. *J. Petrol.* 59 (1), 11–58.
- Weaver, B.L., Tarney, J., 1982. Andesitic magmatism and continental growth. In: Thorpe, R.S. (Ed.), *Andesites: Orogenic andesites and related rocks*. John Wiley & Sons, New York.
- Yogodzinski, G.M., Kelemen, P.B., 1998. Slab melting in the Aleutians: implications of an ion probe study of clinopyroxene in primitive adakite and basalt. *Earth Planet. Sci. Lett.* 158 (1), 53–65.
- Zhu, D.-C., Wang, Q., Cawood, P.A., Zhao, Z.-D., Mo, X.-X., 2017. Raising the Gangdese Mountains in southern Tibet. *J. Geophys. Res.: Solid Earth* 122 (1), 214–223.
- Zimmer, M.M., Plank, T., Hauri, E.H., Yogodzinski, G.M., Stelling, P., Larsen, J., Singer, B., Jicha, B., Mandeville, C., Nye, C.J., 2010. The role of water in generating the Calc-alkaline trend: new volatile data for Aleutian magmas and a new Tholeiitic index. *J. Petrol.* 51 (12), 2411–2444.